PROCEEDINGS OF SCIENCE

Observation of top-quark pair production in heavy-ion collisions with the ATLAS detector

Malak AIT TAMLIHAT[a,*] **on behalf of the ATLAS Collaboration**

[a] *Mohammed V University in Rabat, Faculty of Sciences, 4 av. Ibn Battouta, B.P. 1014, R.P. 10000 Rabat, Morocco*

E-mail: malak.ait.tamlihat@cern.ch

Measurements of top-quark pairs in heavy-ion collisions are anticipated to offer new insights into nuclear parton distribution functions and to provide unique information about the time evolution of strongly interacting matter. We report the observation of top-quark pair production in proton-lead (p+Pb) collisions at the center-of-mass energy of 8.16 TeV with the ATLAS experiment at the LHC. Top-quark pair is studied in the lepton+jets and dilepton channels, and the nuclear modification factor for top-quark pairs is measured for the first time. We also present the first observation of top-quark production in lead-lead (Pb+Pb) collisions at the center-of-mass energy of 5.02 TeV, measured in the $e\mu$ final state with a significance of 5.0 standard deviations. The results are compared with theoretical predictions based on different nuclear PDF sets.

The European Physical Society Conference on High Energy Physics (EPS-HEP2025)
7-11 July 2025
Marseille, France

*Speaker

© Copyright owned by the author(s) under the terms of the Creative Commons Attribution-NonCommercial-NoDerivatives 4.0 International License (CC BY-NC-ND 4.0).
All rights for text and data mining, AI training, and similar technologies for commercial purposes, are reserved.
ISSN 1824-8039. Published by SISSA Medialab.
© Copyright 2025 CERN for the benefit of the ATLAS Collaboration. Reproduction of this article or parts of it is allowed as specified in the CC-BY-4.0 license.

PoS(EPS-HEP2025)196

1. Introduction

The heavy-ion (HI) collisions at TeV-scale energies delivered by the Large Hadron Collider (LHC) at CERN have enabled the study of elementary particle production in lead–lead (Pb+Pb) and proton–lead (p+Pb) systems. Among the particles predicted by the Standard Model (SM), only two remain to be directly observed in Pb+Pb collisions: the Higgs boson and the top quark. While the Higgs boson production cross section is too low to allow its observation in Pb+Pb collisions at the LHC, the observation of top-quark production is within reach. The top quark is the heaviest known elementary particle, with a mass of $m_t = 172.52 \pm 0.33$ GeV [1]. The top quark is extremely short-lived, decaying almost exclusively via $t \to Wb$. The W boson subsequently decays either leptonically ($W \to \ell\nu_\ell$, where $\ell = e, \mu$) or hadronically ($W \to q\bar{q}'$) [2]. At the LHC, top quarks are predominantly produced in top quark–antiquark ($t\bar{t}$) pairs via gluon–gluon fusion, as shown in Figure 1, with their production rate significantly exceeding that of single top quarks [3].

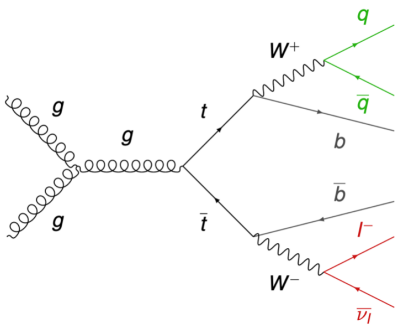

Figure 1: Feynman diagram for top-quark pair production via gluon-gluon fusion, with subsequent decays of the top quark and antiquark into W bosons and b quarks.

2. Top-quark pair production in p+Pb collisions

2.1 Analysis strategy

In p+Pb collisions, top quarks provide a novel probe of nuclear parton distribution functions (nPDFs) in a kinematic region that remains poorly constrained by other experimental data [4, 5]. Using data collected in 2016 from p+Pb collisions at a center-of-mass energy per nucleon pair of $\sqrt{s_{\mathrm{NN}}} = 8.16$ TeV with the ATLAS detector [6], corresponding to an integrated luminosity of 165 nb^{-1}, the $t\bar{t}$ production cross section is measured. The measurement is performed by reconstructing top-quark pairs in both the ℓ+jets and dilepton decay channels, using final states that include electrons, muons, and jets. Events are selected using single-electron or single-muon triggers with a minimum transverse momentum threshold of $p_{\mathrm{T}} > 15$ GeV [7, 8]. Electrons and muons are required to satisfy the "Medium" identification and isolation criteria [9, 10], and must have transverse momentum $p_{\mathrm{T}} > 18$ GeV and pseudorapidity $|\eta| < 2.47$ for electrons and $|\eta| < 2.5$ for muons. Jets are reconstructed using the anti-k_{t} algorithm [11] with a radius parameter of $R = 0.4$. The reconstructed jets are required to have a transverse momentum of $p_{\mathrm{T}} > 20$ GeV and a pseudorapidity of $|\eta| < 2.5$. Six signal regions (SRs) are defined based on the variable $H_{\mathrm{T}}^{\ell,j}$,

PoS(EPS-HEP2025)196

the scalar sum of the transverse momenta of the selected leptons and jets. In the ℓ+jets channel, events are categorized according to lepton flavor and b-jet multiplicity into four SRs: $1\ell 1b$ e+jets, $1\ell 2b_{\text{incl}}$ e+jets, $1\ell 1b$ μ+jets, and $1\ell 2b_{\text{incl}}$ μ+jets. A minimum of four jets is required for these events. In the dilepton channel, events must contain two opposite-sign leptons with an invariant mass $m_{\ell\ell} > 15\,\text{GeV}$ and at least two jets. These events are further divided into two SRs based on b-jet multiplicity: $2\ell 1b$ (exactly one b-jet) and $2\ell 2b_{\text{incl}}$ (at least two b-jets). The contribution from fake leptons is estimated using the Matrix Method (MM) [12], while all other background processes are modeled using Monte Carlo (MC) simulations [13, 14]. The signal strength $\mu_{t\bar{t}}$, defined as the ratio of the observed $t\bar{t}$ cross section to the Standard Model expectation, is measured using a profile-likelihood fit [15] to the $H_{\text{T}}^{\ell,j}$ distributions. The $H_{\text{T}}^{\ell,j}$ distributions predicted by the fit are shown in Figure 2 for the six SRs.

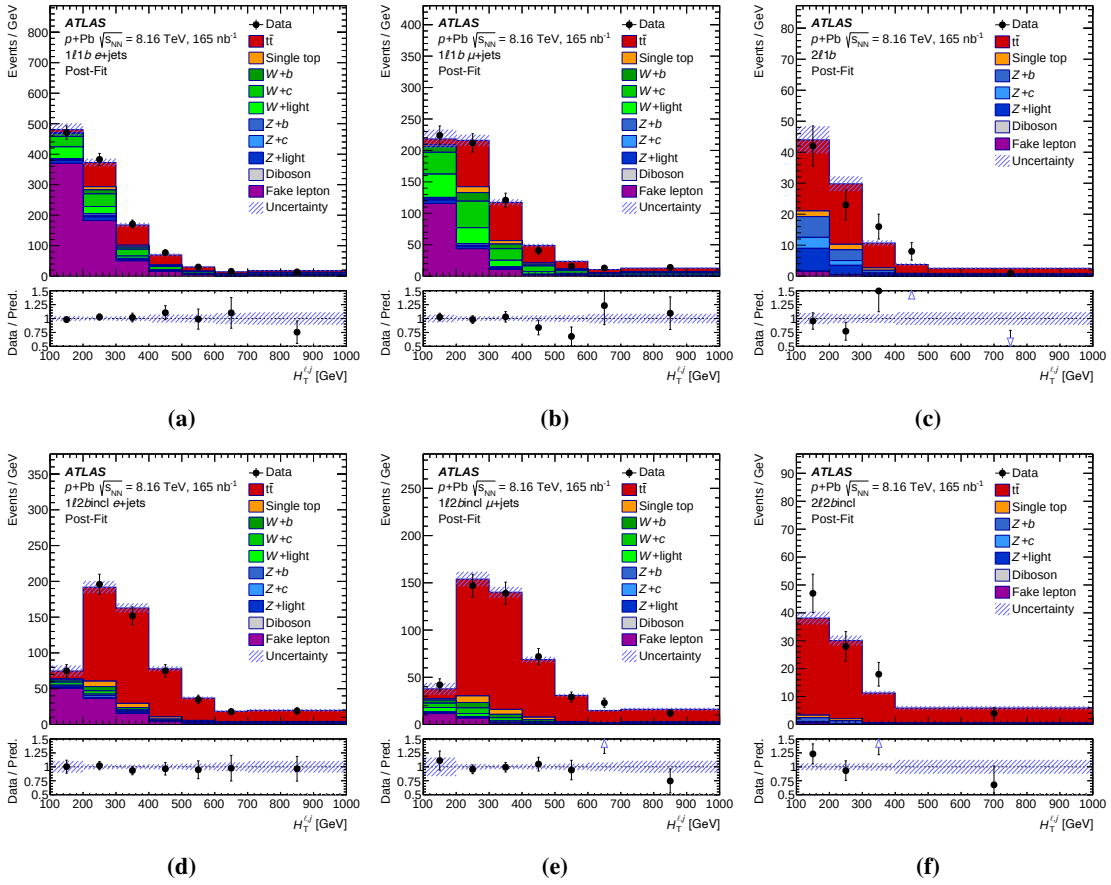

Figure 2: Post-fit distributions of $H_T^{\ell j}$ in the six signal regions (SRs): (a) e+jets $1\ell 1b$, (b) μ+jets $1\ell 1b$, (c) dilepton $2\ell 1b$, (d) e+jets $1\ell 2b$incl, (e) μ+jets $1\ell 2b$incl, and (f) dilepton $2\ell 2b$incl. The total uncertainties are represented by the hatched bands. The bottom panels show the data-to-prediction ratio [16].

2.2 Results

The measured value of $\mu_{t\bar{t}}$ is then translated into the inclusive $t\bar{t}$ production cross section, yielding:

$$\sigma_{t\bar{t}}^{p+\text{Pb}} = 58.1 \pm 2.0\,(\text{stat.})\,^{+4.8}_{-4.4}\,(\text{syst.})\,\text{nb} = 58.1^{+5.2}_{-4.9}\,(\text{tot.})\,\text{nb}. \quad (1)$$

PoS(EPS-HEP2025)196

The total relative uncertainty is 9%. The nuclear modification factor $R_{p\mathrm{A}}$ is defined as the ratio of the $t\bar{t}$ cross section in p+Pb collisions to that in pp collisions [18], scaled by the lead mass number $A_{\mathrm{Pb}} = 208$, and quantifies differences between the two systems. It is measured to be:

$$R_{p\mathrm{A}} = 1.090 \pm 0.039\ (\mathrm{stat.})\ ^{+0.094}_{-0.087}\ (\mathrm{syst.}) = 1.090 \pm 0.100\ (\mathrm{tot.}). \tag{2}$$

Figure 3 shows the comparison of the measured $\sigma_{t\bar{t}}$ and $R_{p\mathrm{A}}$ with other experimental results and theoretical predictions. The measured cross section is consistent with the CMS measurement in p+Pb collisions at $\sqrt{s_{\mathrm{NN}}} = 8.16$ TeV [17], and with the precise ATLAS+CMS combination in pp collisions at $\sqrt{s} = 8$ TeV [18], extrapolated to the centre-of-mass energy of this measurement and scaled by A_{Pb} to the p+Pb system. The result of $R_{p\mathrm{A}}$ is also consistent with the geometric expectation from pp collisions within uncertainties. The measured $\sigma_{t\bar{t}}^{p+\mathrm{Pb}}$ and $R_{p\mathrm{A}}$ values are also compatible with theoretical predictions obtained using four different nuclear PDF sets: EPPS21 [19], nCTEQ15HQ [20], nNNPDF3.0 [21], and TUJU21 [22].

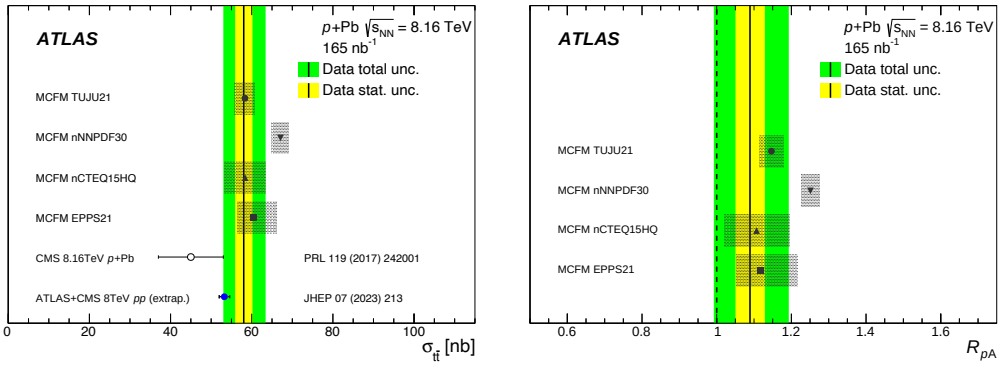

(a) **(b)**

Figure 3: Comparison of (a) the $t\bar{t}$ production cross section and (b) the nuclear modification factor with other measurements and theoretical predictions. The dashed line at $R_{p\mathrm{A}} = 1$ represents the geometric expectation from pp collisions [16].

3. Top-quark pair production in Pb+Pb collisions

3.1 Analysis strategy

In ultra-relativistic Pb+Pb collisions at the LHC, top quarks offer a unique opportunity to probe the properties of the strongly interacting quark–gluon plasma (QGP) [23]. Using the full Run 2 ATLAS Pb+Pb dataset, collected in 2015 and 2018 and corresponding to an integrated luminosity of 1.9 nb^{-1} at a center-of-mass energy of $\sqrt{s_{\mathrm{NN}}} = 5.02$ TeV, the first observation of top-quark pair ($t\bar{t}$) production in heavy-ion collisions is achieved. Top-quark candidates are selected in the electron–muon ($e\mu$) decay channel. Electrons and muons are required to satisfy the "Loose" identification and isolation criteria [9], with transverse momentum thresholds of $p_{\mathrm{T}} > 18$ GeV for electrons and $p_{\mathrm{T}} > 15$ GeV for muons, and pseudorapidity $|\eta| < 2.47$ for electrons and $|\eta| < 2.5$ for muons. Jets are reconstructed using the anti-k_t algorithm [11] with a radius parameter of $R = 0.4$, and jet kinematics are corrected on an event-by-event basis to account for contributions from the underlying

PoS(EPS-HEP2025)196

event (UE). Events are required to contain exactly one electron and one muon of opposite charge, and at least two jets. Two signal regions (SR1 and SR2) are defined based on the transverse momentum of the dilepton system, $p_{\mathrm{T}}^{e\mu}$. SR1 includes events with $p_{\mathrm{T}}^{e\mu} > 40$ GeV, while SR2 corresponds to events with $p_{\mathrm{T}}^{e\mu} \leq 40$ GeV. To suppress contributions from photon-induced processes, events are selected within the 0–80% centrality interval. Backgrounds arising from fake leptons are estimated using data-driven techniques. Additionally, the invariant mass of the $e\mu$ pair, $m_{e\mu}$, is required to be at least 30 GeV to further reduce the fake-lepton background. The signal strength $\mu_{t\bar{t}}$ is obtained using a profile-likelihood fit [15] from a combined fit to the $m_{e\mu}$ distributions. The invariant mass distributions predicted by the fit in the two signal regions are shown in Figure 4.

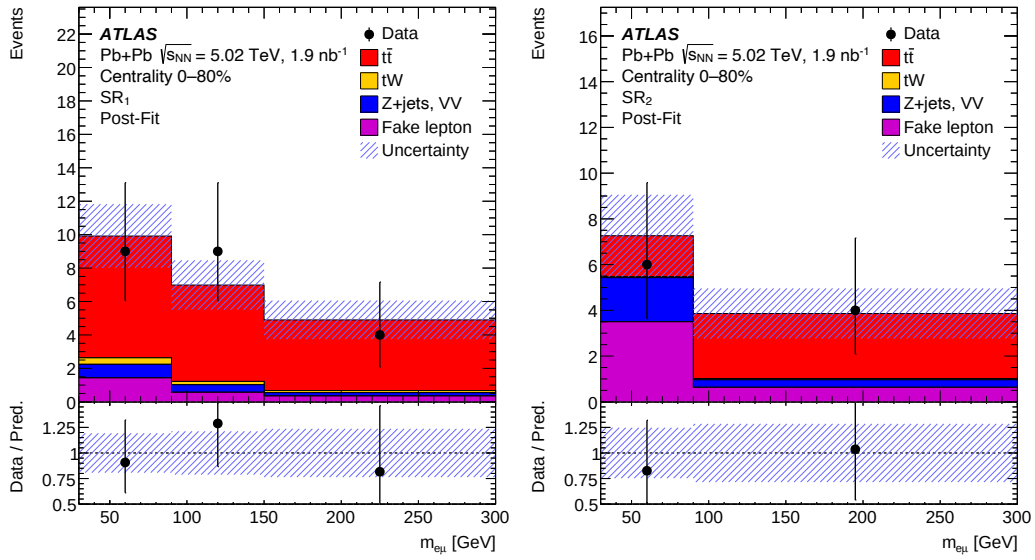

(a) **(b)**

Figure 4: Post-fit distributions of $m_{e\mu}$ in the two signal regions (SRs): (a) SR_1: $p_{\mathrm{T}}^{e\mu} > 40$ GeV, and (b) SR_2: $p_{\mathrm{T}}^{e\mu} \leq 40$ GeV. The total uncertainties are represented by the hatched bands. The bottom panels show the data-to-prediction ratio [24].

3.2 Results

The measured $\mu_{t\bar{t}}$ value is translated into an inclusive top-quark pair production cross section $\sigma_{t\bar{t}}$, using the theoretical prediction $\sigma_{t\bar{t}}^{\mathrm{th}}$ derived for the 0–100% centrality interval. The theoretical cross section is calculated in pp collisions at $\sqrt{s_{\mathrm{NN}}} = 5.02$ TeV and scaled by the square of the lead mass number (A_{Pb}^2). The measured inclusive $t\bar{t}$ production cross section in Pb+Pb collisions is:

$$\sigma_{t\bar{t}}^{\mathrm{Pb+Pb}} = 3.6^{+1.0}_{-0.9}\ (\mathrm{stat.})\ ^{+0.8}_{-0.5}\ (\mathrm{syst.})\ \mu\mathrm{b} = 3.6^{+1.2}_{-1.0}\ (\mathrm{tot.})\ \mu\mathrm{b}. \tag{3}$$

The total relative uncertainty is 31%, dominated by the statistical component of 26%. Figure 5 shows the measured $\sigma_{t\bar{t}}$ compared with the CMS measurement in Pb+Pb collisions at $\sqrt{s_{\mathrm{NN}}} = 5.02$ TeV [25], and with the ATLAS measurement in pp collisions at the same energy, scaled by A_{Pb}^2 [26]. All experimental results are consistent within their uncertainties. The measured cross section is also compared with theoretical predictions using four different nuclear PDF sets:

PoS(EPS-HEP2025)196

EPPS21 [19], nCTEQ15HQ [20], nNNPDF3.0 [21], and TUJU21 [22], with good agreement observed across all predictions.

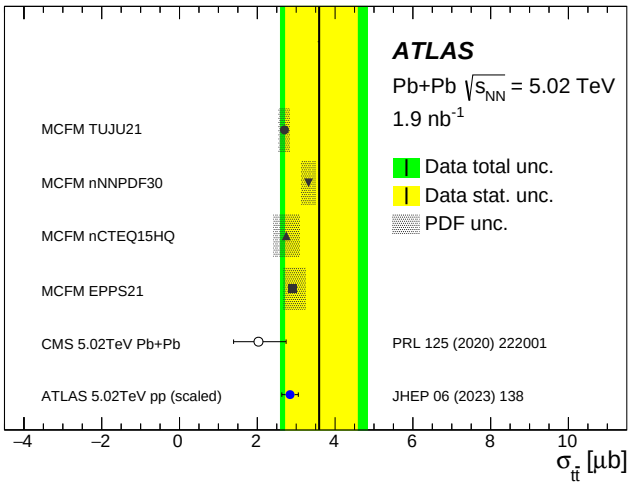

Figure 5: Measurements of the $t\bar{t}$ production cross section compared to other experimental measurements and the theoretical predictions based on four different nuclear PDF sets [24].

4. Conclusion

Top-quark production has been observed in heavy-ion collisions using the ATLAS detector. In p+Pb collisions, the top-quark pair production cross section is measured with a relative uncertainty of 9%, making it the most precise determination of a cross section in nuclear collisions reported to date. The nuclear modification factor for the $t\bar{t}$ process is measured for the first time by ATLAS in p+Pb collisions. Additionally, top-quark production is observed in Pb+Pb collisions using the $e\mu$ channel, with a significance of 5σ, marking the first observation of this process in such collisions. These results open new avenues for the study of nuclear PDFs and the properties of the QGP. With the upcoming High-Luminosity LHC (HL-LHC) runs, significantly larger datasets, along with major improvements in instrumentation, triggers, and reconstruction, will allow differential measurements of top-quark production in heavy-ion collisions.

Acknowledgments

I would like to thank the Moroccan National Center for Scientific and Technical Research (CNRST). I also acknowledge the Moroccan Ministry of Youth, Culture, and Communication, as well as the L'Oréal–UNESCO Foundation, which funded the research project through the "Moroccan Youth Prize" and the "18th L'Oréal–UNESCO For Women in Science (FWIS) Maghreb Prize 2024" programs.

References

[1] ATLAS and CMS collaborations, Phys. Rev. Lett. 132 (2024) 261902.

PoS(EPS-HEP2025)196

[2] Particle Data Group collaboration, PTEP 2022 (2022) 083C01.

[3] A. Giammanco and R. Schwienhorst, Rev. Mod. Phys. 90 (2018) 035001.

[4] D. d'Enterria, K. Krajczár and H. Paukkunen, Phys. Lett. B 746 (2015) 64.

[5] H. Khanpour and S. Atashbar Tehrani, Phys. Rev. D 93 (2016) 014026.

[6] ATLAS Collaboration, 2008 JINST 3 S08003.

[7] ATLAS Collaboration, Eur. Phys. J. C 80 (2020) 47.

[8] ATLAS Collaboration, 2020 JINST 15 P09015.

[9] ATLAS Collaboration, 2019 JINST 14 P12006.

[10] ATLAS Collaboration, Eur. Phys. J. C 81 (2021) 578.

[11] M. Cacciari, G.P. Salam and G. Soyez, JHEP 04 (2008) 063.

[12] ATLAS Collaboration, 2023 JINST 18 T11004.

[13] Sherpa collaboration, SciPost Phys. 7 (2019) 034.

[14] R. Frederix, E. Re and P. Torrielli, JHEP 09 (2012) 130.

[15] K. Cranmer, G. Lewis, L. Moneta, A. Shibata, and W. Verkerke, CERN-OPEN-2012-016.

[16] ATLAS Collaboration, JHEP 11 (2024) 101.

[17] CMS Collaboration, Phys. Rev. Lett. 119 (2017) 242001.

[18] ATLAS and CMS collaborations, JHEP 07 (2023) 213.

[19] K. J. Eskola, P. Paakkinen, H. Paukkunen and C. A. Salgado, Eur. Phys. J. C 82 (2022) 413.

[20] K. Kovarik *et al.*, Phys. Rev. D 93 (2016) 085037.

[21] R. Abdul Khalek *et al.*, Eur. Phys. J. C 82 (2022) 507.

[22] I. Helenius, M. Walt and W. Vogelsang, 29th International Workshop on Deep-Inelastic Scattering and Related Subjects, Santiago de Compostela, Spain (2022).

[23] L. Apolinário, J. G. Milhano, G. P. Salam and C. A. Salgado, Phys. Rev. Lett. 120 (2018) 232301.

[24] ATLAS Collaboration, Phys. Rev. Lett. 134 (2025) 142301.

[25] CMS Collaboration, Phys. Rev. Lett. 125, 222001 (2020).

[26] ATLAS Collaboration, J. High Energy Phys. 06 (2023) 138.

PoS(EPS-HEP2025)196